Structural Analysis using X-Ray Diffraction and FTIR Spectroscopic Studies on Mn²⁺ Substituted CaWO₄ Materials Synthesized by Coprecipitation Method

M. Jaganadha Rao[1,2,*], K.S.R. Murthy[2], Ch. Ravi Shankar Kumar[3],
Anjali Jha[4], G.S.V.R.K. Choudary[5], and M. Chaitanya Varma[2]

[1]Department of General Section, Government Polytechnic, Srikakulam-532005, India
[2]Department of Physics, Institute of Technology, GITAM University, Visakhapatnam-530045, India
[3]Department of Electronics and Physics, Institute of Science, GITAM University, Visakhapatnam-530045, India
[4]Department of Chemistry, Institute of Science, GITAM University, Visakhapatnam-530045, India
[5]Department of Physics, Bhavan's Vivekananda College, Sainikpuri, Secunderabad-500094, India

*Corresponding author: E-mail: mjrphysics1964@gmail.com

Present day technology requires synthesis of materials with low energy consumption, free mercury pollution and its reliability. A novel material with control of crystallite size, composition and simple for white light relies in synthesis of materials. The present focus of article attributes series of manganese doped $Ca_{1-x}Mn_xWO_4$ luminescent materials with co-precipitation method. Reported studies attempts with change in structure of calcium tungstate ($CaWO_4$) are observed with dopants like Eu^{3+}, Eu^{2+}, Tb^{3+}, *etc*. However the effect of Mn^{2+} on structural properties of $CaWO_4$ are quite interesting. The synthesized samples were characterized with X-ray diffraction for lattice parameters, crystallite size and FTIR studies for bonding mechanism of O-W-O stretching and W-O-W bridge bond. Rietveld profile refinement of XRD patterns using MAUD program $Ca_{1-x}Mn_xWO_4$ revealed the Scheelite type structure with C_{4h} point group and I41/a space group. Characterization studies reveal that doping of Mn^{2+} doping upto 0.1 in place of Ca^{2+} will not change the phase of Scheelite structure.

Keywords: CaWO₄, Scheelite structure, Rietveld refinement, FTIR.

INTRODUCTION

For the past few years, there is an exponential growth in the generation of white light sources owing to their great potential for applications in display and lighting. In particular white light emission from a single-phase phosphor is of interest [1]. White-light emitting luminescent materials have gained significant interest in various fields like information display, fluorescent sensors, and optical-recording systems, *etc*. However, producing single phase white-light-emitting materials, which could emit the pure white light is really a challenging task. In this regard, calcium tungstate (CaWO₄) an important optical material, due to its potential applications with electro-optical properties like refractive index, susceptibility, energy gap, *etc*. with Scheelite structure [2] has been selected in the present work.

As a self-activating phosphor, CaWO₄ can emit a high-efficiency blue emission due to the tetrahedral WO_4^{2-} groups

in the host lattices [3]. Tm^{3+}/Ho^{3+}/Yb^{3+} co-doped CaWO₄ materials have been reported to show white upconversion luminescence under the excitation of 980 nm. In this material by doping rare earth elements red colour to blue colour emission has been reported with different synthesis methods [4]. This is based on energy transfer to obtain white light and can be realized by co-doping various luminescent ions into one host. Since the availability of rare earth ions and their cost have limitations for synthesizing such materials, an alternate dopants have to be identified for production of efficient luminescent materials.

Katsumata *et al*. [5] studied X-ray excited optical luminescence from Mn doped spinel (MgAl₂O₄) crystal under CuK_α irradiation. They observed strong luminescence from 2.0 % Mn doped crystal without influence of concentration quenching showing a peak intensity of photoluminescence spectra at λ = 520 nm. The effect of pH of chemical reactants and manganese concentration on luminescence properties of CaMoO₄

nanocrystals have been studied by Dai *et al.* [6]. They observed that lower pH and lower concentration of Mn resulted in uniform nanospheres with narrow size and higher luminescence thermal stability. The band gap value increased with increase in Mn content from 4.47 to 4.78 eV [6].

Pawlikowska *et al.* [7] synthesized pure and manganese doped calcium molybdates ($Ca_{1-x}Mn_xMoO_4$) as well as molybdato-tungstates $(Ca_{1-x}Mn_xMoO_4)_{0.50}(WO_4)_{0.50}$ for $0 < x \leq 0.15$ by solid state reaction and citrate-nitrate combustion methods. They identified that with increase in Mn content in $Ca_{1-x}Mn_x MoO_4$ band gap value decreased upto Mn concentration of 0.10 and with further increase of Mn band gap increased. Whereas in case of $Ca_{1-x}Mn_xMoO_4)_{0.50}(WO_4)_{0.50}$ band gap value decreased with increasing Mn concentration. Li *et al.* [8] observed intense green emission when Zn^{2+} ions are replaced with Mn^{2+} ions in Zn_2GeO_4 synthesized by facile solvothermal process with H_2O/ethylene glycol as solvent. This kind of intense green emission has been attributed to the *d-d* transition ($^4T_1 \rightarrow {}^6A_1$) of Mn^{2+} ions. They also elaborately studied the luminescence mechanisms of Zn_2GeO_4:Mn^{2+} by using density functional theory (DFT).

Similarly, White *et al.* [9] observed a bright green light emission in Mn doped zinc silicate and phosphate where Mn^{2+} ions act as activators. Chan *et al.* [10] showed an increase in photoluminescence intensities in $LiZn_{1-x}PO_4$:Mn_x phosphors with various concentrations of Mn (x = 0.02, 0.04,0.06, 0.08, 0.1, 0.12, 0.14, 0.18, 0.22) upto x = 0.12 and then it decreased as a result of concentration quenching. The emission lines are attributed to transitions of Mn^{2+} ion from ground level $^6A_1(^6S)$ to $^4E (^4D)$, $^4T_2(^4D)$, [$^4A_1(^4G)$, $^4E(^4G)$], $^4T_2(^4G)$ and $^4T_1(^4G)$ excited levels.

Zhang *et al.* [11] tried to explore the optical properties of Mn-doped AWO_4 (A = Ca, Sr, Ba) nanorods synthesized using a modified template-directed methodology under ambient, room-temperature conditions. They identified that presence of Mn^{2+} not only substantially increases the photoluminescent potential of a pristine tungstate material but also reinforces its versatility by adding a desirable magnetic component to its repertoire of properties. Broadband absorption in the range from 350 to 450 nm has been observed by them in UV-visible absorption spectra of as-prepared Mn-doped tungstate nanorods at room temperature, corresponding to $^6A_1 \rightarrow {}^4T_1$ transition associated with the 3*d* states of Mn^{2+} ions. They also observed that the emission peak positions were not affected by the incorporation of Mn ions, implying that the energy gap related to the blue emission within WO_4^{2-} complexes is similarly unaltered by the presence of Mn dopant. However, Mn-doped alkaline-earth metal tungstate nanorod samples clearly showed far greater and enhanced photoluminescent emission intensity as compared with their undoped counterparts, all normalized in terms of concentration. That is, as compared with pure $CaWO_4$ nanorods, Mn-doped $CaWO_4$ nanorods yielded 1.8 times greater luminescence intensity at the major peak position located at 502 nm. The observed increase in luminescence has been partially attributed to the intra-3*d*-shell transitions of Mn^{2+} ions.

Based on the literature, it has been identified that clear understanding of the effect of Mn^{2+} ions on the optical properties of $CaWO_4$ is necessary. This is in fact due to the changes

observed such a increase intensity or shift towards blue light region in Mn doped luminescent materials. In order to understand these in this work, manganese has been selected as dopant in place of calcium in $CaWO_4$ and initially the effect of Mn on structural properties of $CaWO_4$ has been presented.

EXPERIMENTAL

To synthesize nano crystalline $Ca_{1-x}Mn_xWO_4$, each of $Na_2WO_4\cdot2H_2O$, $Ca(NO_3)_2\cdot4H_2O$ and $MnCl_2\cdot4H_2O$ were separately dissolved in deionised water and stirred for 0.5 h to obtain clear homogeneous 1 M solution. Calcium nitrate and manganese chloride are mixed and stirred for 1 h. This solution is added dropwise to sodium tungstate at room temperature resulting in the formation white precipitate under continuous stirring for 2 h. The products were washed with water several times and after final washing with ethanol were dried at 95 ºC for 8 h in hot air oven. The powder thus obtained was subjected to heat treatment at 500 ºC to get single phase.

XRD patterns are recorded at room temperature in the 2θ range of 10º to 80º using PanAlytical, X-Pert pro. XRD patterns of all the samples have been refined according to Rietveld profile refinement procedure using MAUD program 2.8 [12]. Fourier transform infrared (FTIR) spectra measurements are made by Shimadzu IR-Prestige 21 instrument in transmittance method with KBr pellet as IR window in the wave number region of 4000 to 400 cm^{-1}.

RESULTS AND DISCUSSION

X-ray diffraction studies of $Ca_{1-x}Mn_xWO_4$ were illustrated in Fig. 1. All diffraction peaks were found perfectly indexed (JCPDS standards, 41-1431) in conformity with scheelite type tetragonal structure with space group I41/a [13]. The XRD spectra confirm that the products are pure in phase with no other characteristic peaks.
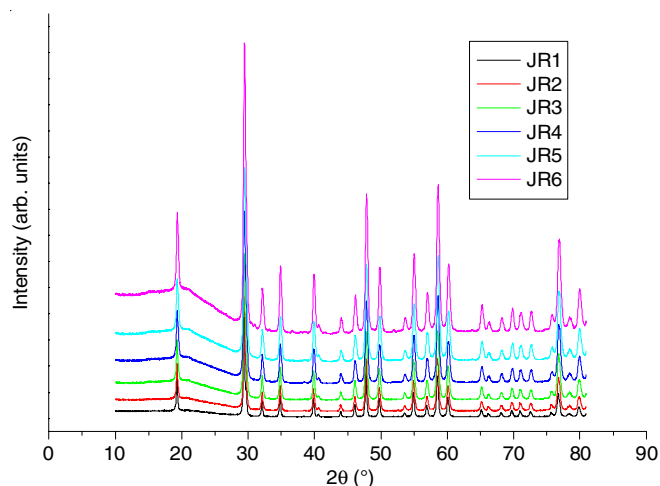

Fig. 1. XRD patterns of $Ca_{1-x}Mn_xWO_4$

The structure of the unit cell manifests that the tungsten atoms are coordinated with four oxygen atoms in order to form tetrahedral [WO_4] clusters, where the tetrahedral angles are minimally distorted. While the calcium atoms are in coordination with eight oxygen atoms, resulting in the formation of [CaO_8] clusters with a deltahedral configuration, a symmetry group

of D_{2d} and a snub-disphenoid polyhedral shape (8 vertices, 12 faces and 18 edges). There is only one type of Ca cationic site with Wyckoff position 4b for Mn^{2+} ion to accommodate, basing on their similar ionic radius of Ca^{2+} [r =1.00 Å for coordination number (C.N.) = 8] and Mn^{2+} (r = 1.10 Å for C.N. = 8).

Secondary phases were not observed in the diffractograms, pointing out that the processes promote only the crystal growth. In addition, the presence of strong and sharp diffraction peaks indicate a typical characteristic of materials, structurally ordered at long-range. The experimental lattice parameters and unit cell volumes were calculated using the Rietveld refinement method and the Maud program. Fig. 2 illustrates that the structural refinements are related to $CaWO_4$. The refinement technique is employed with reference to the least-squares approach, where the theoretical peak profiles are adjusted up to the convergence with the measured profiles. The Rietveld refinement method is endowed with several advantages over the conventional quantitative analysis methods, including usage of pattern-fitting algorithms and all lines of each crystallographic phase are explicitly are taken into account (even those overlapped lines). Thus, it is not necessary to decompose the patterns into separate Bragg peaks. The use of all reflections in a pattern, rather than just the strongest ones, minimizes the uncertainty in the derived weight fractions and the effects of preferred orientation, primary extinction and non-linear detection systems. Also, the structural refinements can be optimized using the Rietveld texture and stress analyses. The difference between the measured and calculated patterns is considered to be one way to verify the success of the refinement. In the Rietveld refinements, the measured diffraction patterns were well suited with Crystallographic Information File (CIF) 9009628 [14].
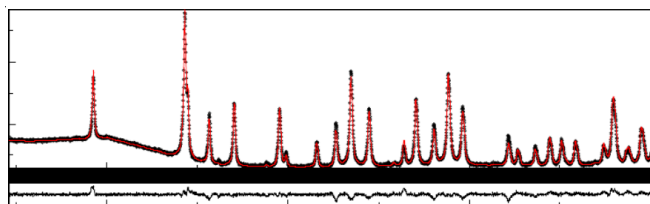

Fig. 2. Rietveld refined pattern of $CaWO_4$

The Rietveld refined results can be assumed to be mostly desirable as $R_w < 10$ % (pertaining to tetragonal, orthorhombic, rhombohedral and hexagonal structures) and the low χ^2 values. These results from Rietveld refinements are displayed in Table-1. In this table, the fit parameters (R_{wnb} and χ^2) suggest that the refinement results are very reliable. It is interesting to note that there are considerable variations in the atomic positions related to the oxygen atoms, while calcium and tungsten atoms

maintain their fixed positions within the structure. These results obviously imply the existence of structural distortions in the $[CaO_8]$ and $[WO_4]$ clusters of $CaWO_4$ materials.

In this case, it was noticed that the lattice parameters and unit cell volumes are very close to the published in literature. The small variations between these values can be attributed to the peculiarity of each synthesis method, where the experimental variables (temperature, time processing, heating rate, solvents, *etc*.) are capable of influencing the organization of $[CaO_8]$ and $[WO_4]$ clusters within the Scheelite structure. These variables can cause the formation or reduction of structural defects (oxygen vacancies, distortion on the bonds, stresses and strains on the crystalline lattice) in the materials.

Interpretation of vibration studies for all complexes with change in concentration of manganese are illustrated in Fig. 3. All the vibrations of these complexes were in assigned regions in functional and fingerprint regions as listed in Table-2.
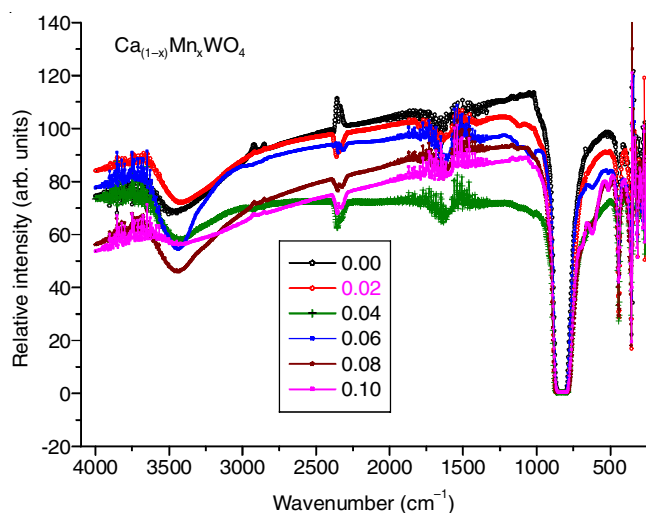

Fig. 3. FTIR spectra of $Ca_{1-x}Mn_xWO_4$

With an increase in concentration in respective proportions for calcinations in stoichiometric proportions there is greater tendency of manganese nitrate with shift in wavenumber increased by 15 cm^{-1} in formation of complex. However, there is no proportional change in wave numbers of manganese oxide. There is reduction in W-O-W stretching of 12 cm^{-1} with bridge bonds and enhancement to maximum of 19 cm^{-1} with increase in concentration. There is maximum increase O-H in all the complexes with increase in concentration require the samples to be calcinated. The absence of carbonyl peak around 1730 cm^{-1} indicates removing of oxalate during the washing process. The two absorption bands at 869-848 and 441 cm^{-1} belong to the O-W-O stretching and W-O bending vibrations of WO_4 tetra-

TABLE-1
LATTICE PARAMETERS OBTAINED FROM RIETVELD REFINEMENT OF XRD PATTERNS OF $Ca_{1-x}Mn_xWO_4$

x	Lattice constant (Å)		Crystallite size (nm)	Microstrain	Rwp (%)	χ^2
	'a'	'c'				
0	5.2588	11.4100	991.95	6.197×10^{-4}	7.9924	2.55
0.02	5.2611	11.4154	594.23	1.544×10^{-3}	9.8599	2.49
0.04	5.2556	11.4037	500.54	1.449×10^{-3}	7.8630	2.12
0.06	5.2560	11.4034	670.26	1.285×10^{-3}	8.9961	2.55
0.08	5.2525	11.3945	533.34	1.718×10^{-3}	9.8437	2.64
0.10	5.2534	11.3957	774.94	1.541×10^{-3}	8.9311	3.46

TABLE-2
FTIR STUDIES OF $Ca_{1-x}Mn_xWO_4$

x	M-N band	W-O band	O-W-O stretching	W-O-W bridge bond	O-H stretch
0	340.9	441.7	804.3	843.8	3176
0.02	354.0	441.0	788.0	869.0	3379
0.04	356.0	441.0	788.0	–	3361
0.06	354.0	441.0	800.0	850.0	3271
0.08	356.0	441.0	788.0	862.0	3271
0.10	–	441.0	796.0	846.0	–

hedron [8]. The peaks around 3400 to 3200 cm^{-1} correspond to stretching vibration of O-H groups , which corresponds to the water molecules physically absorbed by the KBr pellets and the compounds. The bonds at 700 cm^{-1} which has been observed for Mn = 0.1 compound is related to asymmetrical stretching vibrations of W-O bond in the $(W_2O_4)_n$. With the addition of Mn in $CaWO_4$, there is another peak, which appears to be increasing in intensity and is around 660-620 cm^{-1} indicates the presence of stretching vibration of Mn-O bond. As the concentration increases there is reduction in intensity favoring the bonding of complexes. From the variation in the peaks positions and appearance of additional peaks it can be stated that Mn^{2+} ions are entering into the Scheelite latttice in place of Ca^{2+} ions.

Conclusion

Analysis of $Ca_{1-x}Mn_xWO_4$ for structure and optical properties with manganese were synthesized using co-precipitation method. Initially with increase in Mn^{2+} concentration the volume of the scheelite structure has been observed to increase but further increase in Mn^{2+} led to decrease in the volume. This clearly establishes that cations are adjusting themselves within the structure maintaining the scheelite tetragonal phase. FTIR spectra of all the samples also establish the single phase tetragonal structure with an additional requirement to heat at higher temperatures than 500 °C. This study clearly shows that Mn^{2+} doping upto 0.1 will not lead to any change in phase of $CaWO_4$.

CONFLICT OF INTEREST

The authors declare that there is no conflict of interests regarding the publication of this article.

REFERENCES

1. Y. Zhang, W. Gong, J. Yu, H. Pang, Q. Song and G. Ning, *RSC Adv.*, **5**, 62527 (2015);
https://doi.org/10.1039/C5RA12502B.
2. C. Cui, J. Bi and D. Gao, *Mater. Lett.*, **62**, 2222 (2008);
https://doi.org/10.1016/j.matlet.2007.11.057.
3. A. Phuruangrat, T. Thongtem and S. Thongtem, *J. Exp. Nanosci.*, **5**, 263 (2010);
https://doi.org/10.1080/17458080903513276.
4. M.L. Pang, J. Lin, S.B. Wang, M. Yu, Y.H. Zhou and X.M. Han, *J. Phys.: Condens. Matter*, **15**, 5157 (2003);
https://doi.org/10.1088/0953-8984/15/29/327.
5. T. Katsumata, S. Minowa, T. Sakuma, A. Yoshida, S. Komuro and H. Aizawa, *ECS Solid State Lett.*, **3**, R23 (2014);
https://doi.org/10.1149/2.0011407ssl.
6. Q. Dai, G. Zhang, P. Liu, J. Wang and J. Tang, *Inorg. Chem.*, **51**, 9232 (2012);
https://doi.org/10.1021/ic3006663.
7. M. Pawlikowska, H. Fuks and E. Tomaszewicz, *Ceram. Int.*, **43**, 14135 (2017);
https://doi.org/10.1016/j.ceramint.2017.07.154.
8. Y. Li, A. Zhao, C. Chen, C. Zhang, J. Zhang and G. Jia, *Dyes Pigments*, **150**, 267 (2018);
https://doi.org/10.1016/j.dyepig.2017.12.021.
9. J.W. Hess Jr., J.R. Sweet and W.B. White, *J. Electrochem. Soc.*, **121**, 142 (1974);
https://doi.org/10.1149/1.2396809.
10. T.-S. Chan, R.-S. Liu and I. Baginskiy, *Chem. Mater.*, **20**, 1215 (2008);
https://doi.org/10.1021/cm7028867.
11. F. Zhang, Y. Yiu, M.C. Aronson and S.S. Wong, *J. Phys. Chem. C*, **112**, 14816 (2008);
https://doi.org/10.1021/jp803611n.
12. M.I. Kay, B.C. Frazer and I. Almodovar, *J. Chem. Phys.*, **40**, 504 (1964);
https://doi.org/10.1063/1.1725144.
13. R.M. Hazen, L.W. Finger and W.W. Mariathasan, *J. Phys. Chem. Solids*, **46**, 253 (1985);
https://doi.org/10.1016/0022-3697(85)90039-3.
14. X. Lai, Y. Wei, D. Qin, Y. Zhao, Y. Wu, D. Gao, J. Bi, D. Lin and G. Xu, *Integr. Ferroelectr.*, **142**, 7 (2013);
https://doi.org/10.1080/10584587.2013.780145.